Controlled TiO_2 Nanotube Arrays as an Active Material for High Power Energy-Storage Devices

Journal of The Electrochemical Society, **156** (7) A584-A588 (2009)
0013-4651/2009/156(7)/A584/5/$25.00 © The Electrochemical Society

Controlled TiO_2 Nanotube Arrays as an Active Material for High Power Energy-Storage Devices

Min Seok Kim,[a] Tae-Woo Lee,[b] and Jong Hyeok Park[a,z]

[a]*Department of Chemical Engineering, Sungkyunkwan University, Suwon 440-746, Republic of Korea*
[b]*Department of Materials Science and Engineering, Pohang University of Science and Technology, Pohang, Gyeongbuk 790–784 Korea*

There have been numerous studies of the electrode materials of electric double-layer capacitors (EDLCs), such as activated carbons, carbon nanotubes, and other carbon-based materials which have a high specific surface area. Of the materials being developed for EDLCs, activated carbon remains the most promising because of its low cost and high specific capacitance (~200 F/g). However, the widespread commercial use of activated carbon is impaired by its low volumetric capacitance, which results from its low density. In this study, the charge-storage behavior of TiO_2 nanotube arrays from an electric double layer was investigated. The specific capacitances of the TiO_2 nanotube arrays were greatly influenced not only by their crystalline structure, but also by the electrolyte composition. The volumetric capacitance of the TiO_2 nanotube arrays was more than 1.8 times higher than that of activated-carbon-based EDLCs in a water-based electrolyte.
 [DOI: 10.1149/1.3129682]

Manuscript submitted February 26, 2009; revised manuscript received April 15, 2009. Published May 13, 2009.

Electrochemical capacitors (ECs) have mainly been used in high power energy-storage devices, for example, as power enhancement and primary or hybrid power sources combined with batteries and fuel cells for hybrid electric vehicles or fuel-cell electric vehicles.[1] They are generally classified into two categories, depending on the charge-storage mechanism. First, in electric double-layer capacitors (EDLCs), the performance is correlated with the specific surface area of the activated carbon (AC), being also influenced by other parameters such as the pore size.[2,3] Capacitors in the other class, called redox capacitors, are based on materials with pseudocapacitance characteristics, such as conducting compounds[4,5] or other metal-oxide-based inorganic materials.[6,7] In the case of EDLCs, carbon-based materials with a high specific surface area have been recognized as the most promising candidates for commercialization. The energy-storage mechanism in this case is mainly based on the accumulation of charge in the double layer formed at the electrode/electrolyte interface.[8] In general, the specific capacitance is in the range of 10–30 $\mu F/cm^2$.[9]

Generally, the specific capacitance of EDLCs depends not only on the specific surface area of the AC, but also on other parameters, such as the pore size.[2,3,10] For a high specific capacitance, the pore size in ACs should fit well with the size of the ions in the electrolyte. Although ACs can be prepared with a specific surface area as high as 3000 m^2/g by extensively developing their porosity, they usually possess a very wide pore size distribution, with some of the pores not participating in the formation of the double layer.[9]

It is well known that electric double-layer charge storage is mainly produced by the adsorption of ions on the surface of the electrode material.[11] Therefore, nanostructured materials can provide a relatively short ion-diffusion length to improve the utilization of the electrode surface area at a high power density.[12] Recently, highly ordered, vertically oriented TiO_2 nanotube arrays fabricated by potentiostatic anodization have been developed, which constitute a material architecture that offers a large internal surface area without a concomitant decrease in the geometric and structural orders.[13-15] This nanostructured material with a regular pore size can significantly improve the interfacial ion movement and charge transfer as compared with compact thin films or highly porous materials such as AC. Recently, Xie et al. reported the preparation of a TiO_2 nanotube array embedded by electroactive nickel oxide to form a NiO/TiO_2 nanotube composite, which could be used as a functional electrode material for ECs. In their study, the neat TiO_2 nanotube arrays showed very poor capacitive behavior in the base electrolyte.[16] More recently, Fabregat-Santiago et al. reported a high capacitance of TiO_2 nanotube arrays induced by electrochemical intercalation.[17]

In this study, the EDLC-type charge-storage behavior, charge–discharge behavior, and long-term stability of TiO_2 nanotube arrays were investigated. It was found that the nanotube array itself can participate in the formation of an electric double layer. However, the charge-storage behavior was greatly affected by the crystallinity of the TiO_2 nanotube arrays, tube length, and electrolyte acidity.

Experimental

Titanium foils (0.25 mm thick, 99.5% pure) were purchased from Alfa Aesar (Ward Hill, MA). Before its anodization, the titanium foil was ultrasonically cleaned in distilled water and then in acetone for 10 min each. The foil was then dried in a N_2-filled oven. TiO_2 nanotubes were prepared in an aqueous solution made by mixing acetic acid (CH_3COOH) and 0.5 wt % HF at a concentration ratio of 1:7. The addition of acetic acid results in more mechanically robust nanotubes without changing their shape and size.[17]

The TiO_2 nanotube arrays were fabricated by the potentiostatic anodization of a Ti foil at 20 V (15°C) for several hours. The anodization was conducted with the magnetic agitation of the electrolyte, which reduces the thickness of the double layer at the metal/electrolyte interface and ensures a uniform local current density and temperature over the Ti electrode surface. After anodization, they were immediately rinsed with distilled water and then dried in a N_2 stream. They were annealed at various temperatures for 6 h with heating and cooling rates of 10°C/min in an O_2 atmosphere to crystallize the tube walls.

Field-emission-scanning electron microscope was used to investigate the surface morphology and film thickness of the TiO_2 nanotube arrays. Cyclic voltammetry measurements were conducted in a three-electrode cell consisting of a three-neck 100 mL beaker equipped with a reference electrode (Ag/AgCl), counter electrode (Pt spade), and working electrode (TiO_2 nanotube arrays). Two different aqueous solutions (1 M HCl and 1 M NaOH) were used as an electrolyte. Measurements were carried out using a computer-controlled potentiostat/galvanostat (CHI-66) to determine the electrochemical properties of the electrode. To calculate the weight of the TiO_2 nanotube arrays, we used the following equation[18]

$$\begin{aligned}\text{weight of the nanotube arrays} &= \text{electrode area} \times \text{tube height (from SEM)} \\ &\times (1\text{-porosity of the } TiO_2 \text{ nanotube arrays}) \\ &\times \text{density of } TiO_2 \ (4\ g/cm^3)\end{aligned}$$

[z] E-mail: lutts@skku.edu

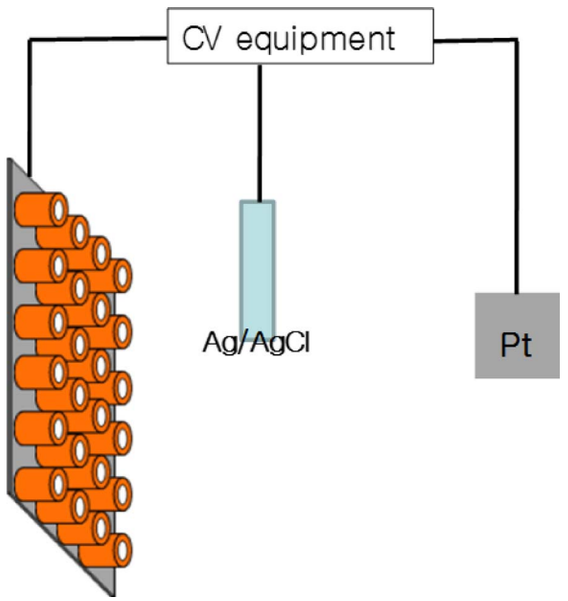

Figure 1. (Color online) Principle of a TiO_2 nanotube-based EDLC.

Results and Discussion

A schematic representation of the TiO_2 nanotube arrays and the electrolytic solution is shown in Fig. 1. During the charging process, the negative electrode attracts the positively charged cations, whereas the anions are accumulated on the surface of the positive electrode. Figure 2 shows the scanning electron microscope (SEM) images of the TiO_2 nanotube arrays with a length of ~400 nm. The pore diameter was about 75 nm and the wall thickness was approximately 12 nm. The cyclic voltammograms (CVs) of the crystalline TiO_2 nanotube arrays in 1 M HCl and 1 M KOH are shown in Fig. 3a and b, respectively. After the anodizing process, they were annealed at 400°C for 6 h to crystallize the tube walls. For the electrode in acid and base electrolytes, the CV curves are close to an ideal rectangular shape, corresponding to EDLC-type energy storage. As can be seen in Fig. 3a, the current densities increased linearly as a function of the voltage scan rate, and the shapes were maintained at a high voltage scan rate, indicating good power properties.[8] Generally, from a series of ACs with different pore sizes in various electrolytes, there is no linear relationship between the specific surface area and the capacitance because some parts of the pores are not accessible to the ions in the electrolytes.[19] However, because the inner pore diameter of the anodized TiO_2 nanotube arrays and the internanotube distance were about 80 and 10 nm, respectively, all of the ions in the electrolytes can access the entire surface of the nanotube arrays.

Figure 3b shows the CV characteristics of the TiO_2 nanotube arrays in a base solution (1 M KOH). When compared with Fig. 3a, the CV diagrams are very noisy and the current densities were one-sixth of those in the acid electrolyte. It has been reported that the use of base electrolytes increases the concentrations of physisorbed OH^- ions on semiconductors, which participate in the hole-trapping process.[20,21] We could expect the physisorbed OH^- ions on the TiO_2 nanotube arrays to interfere with the formation of the electric double layer, resulting in a lower specific capacitance. The CV characteristics of the TiO_2 nanotube arrays with an amorphous phase in 1 M HCl were also evaluated, as shown in Fig. 3c. When compared with Fig. 3a, the current densities at the same scan rates are greatly reduced, indicating that the conductivity of the unannealed TiO_2 nanotube arrays is lower than that of the annealed arrays.

The complete kinetic characterization of the absorption/desorption of ions and electron transportation is provided by impedance measurements. The impedance spectra of the TiO_2 nanotube arrays with different crystalline structures are shown in Fig. 4. The electrodes were potentiostatically charged at several potentials until equilibrium was reached. Generally, the impedance spectrum consists of three distinct parts which are dependent on the frequency range. The high frequency region identifies the electrolyte properties, while the impedance response in the midfrequency region is associated with the electrode/electrolyte interface process.[22] At low frequency, the response in the shape of a 90° straight line in the ideal case resembles that of the pure capacitance.[23] In the case of pseudocapacitive materials, generally, due to the difference in the oxidation levels, nonidentical spectra are obtained over the various potential ranges.[24] As can be seen in Fig. 4a, very similar spectra, independent of the applied potential, were observed in the case of the crystalline TiO_2 nanotube arrays. The almost vertical dependence of the imaginary part indicates good capacitive behavior without any diffusion limitations.[25] The most important features of the impedance spectra of the amorphous TiO_2 nanotube arrays in Fig. 4b are the low frequency (real axis) impedance intercept values, reflecting the high cell resistance. From Fig. 4a and b, we can conclude that the crystalline TiO_2 nanotube arrays have a much lower resistance than the amorphous TiO_2 nanotube arrays. These increased resistances are attributed to their low specific capacitances.

The charge–discharge tests of the crystalline TiO_2 nanotube arrays were performed at constant current densities of between −0.2 and 0.7 V. The typical potential profiles of the charge/discharge process are shown in Fig. 5. During the charge and discharge steps, almost linear behavior of the electrode potential is observed, as would be expected from the CV curves. The results shown in Fig. 5 demonstrate that the TiO_2 nanotube arrays exhibit a very similar response to the AC-based EDLCs. The variation in the discharge capacitance of the TiO_2 nanotube arrays as a function of the cycle number is given in Fig. 6. One cycle including the charge and dis-

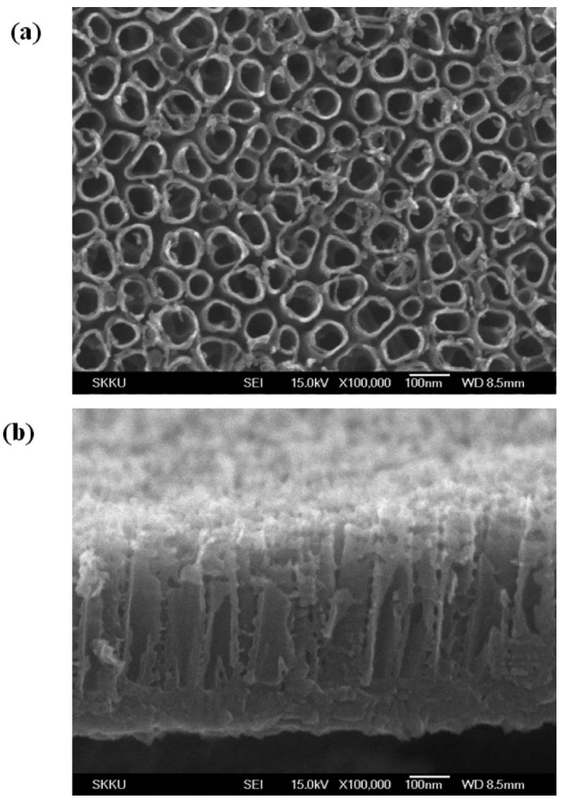

Figure 2. The SEM micrographs of the TiO_2 nanotube arrays: (a) Top view and (b) side view.

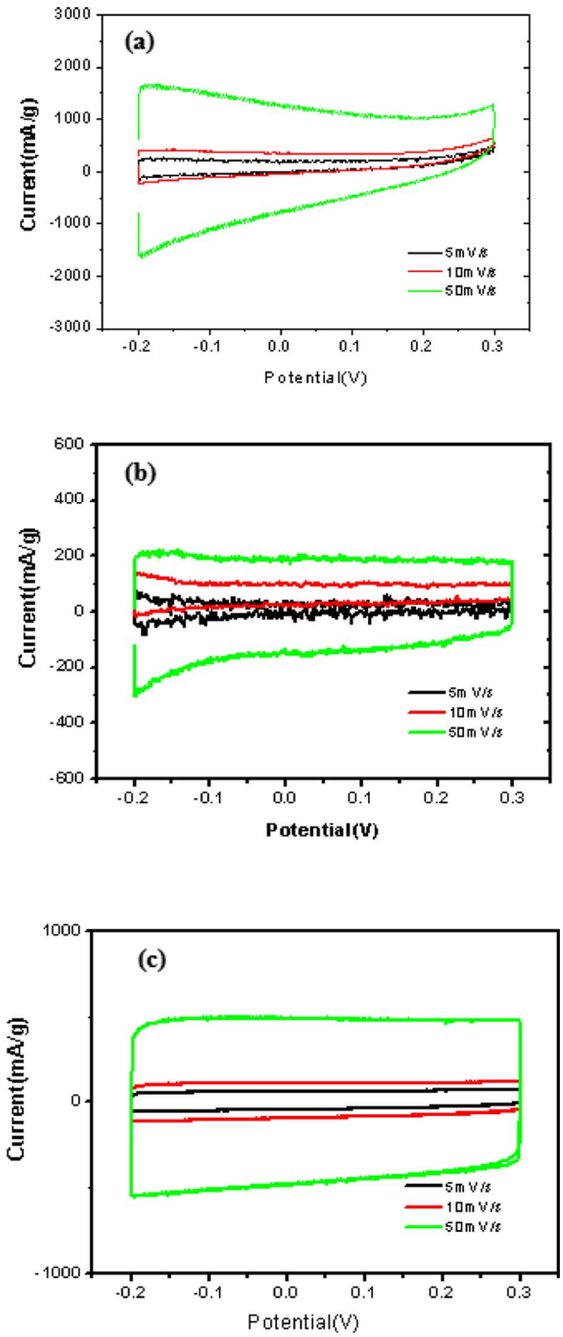

Figure 3. (Color online) The (a) CVs of TiO_2 nanotube arrays annealed at 400°C in 1 M HCl electrolyte, (b) CVs of TiO_2 nanotube arrays annealed at 400°C in 1 M NaOH electrolyte, and (c) CVs of TiO_2 nanotube arrays without thermal annealing in 1 M HCl electrolyte.

charge steps takes approximately 20 s. The capacitance can be maintained at nearly 100% after 1000 cycles, representing very high long-term stability.

As can be seen in Fig. 2a and c, the charge-storage characteristics were strongly influenced by the crystal structure of the TiO_2 nanotube arrays. Therefore, the effects of the annealing temperature on the charge-storage behaviors were investigated. The Ti foil was anodized at 15°C and 20 V for 3 h and then annealed for a further 6 h at a temperature of either 400, 500, or 600°C. The as-anodized titania nanotubes are amorphous and are subsequently crystallized

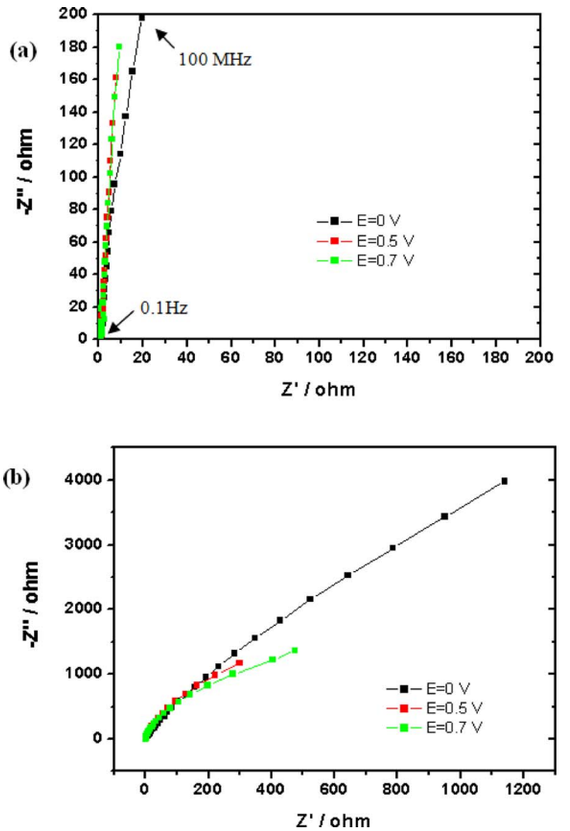

Figure 4. (Color online) Impedance spectra of (a) TiO_2 nanotube arrays thermal annealed at 400°C in 1 M HCl and (b) TiO_2 nanotube arrays without thermal annealing in 1 M HCl.

by the high temperature annealing. In our previous work, the anatase phase started to appear at a temperature of 300°C. A weak rutile phase peak appeared in the X-ray diffraction pattern at a temperature near 450°C.[26] Figure 7 shows the CV curves of the TiO_2 nanotube arrays thermally annealed at different temperatures at a scan rate of 50 mV/s. The specific current densities were strongly dependent on the annealing temperature. As the annealing temperature was increased above 400°C, the specific capacitance decreased gradually. This might be due to the fact that, as the annealing temperature

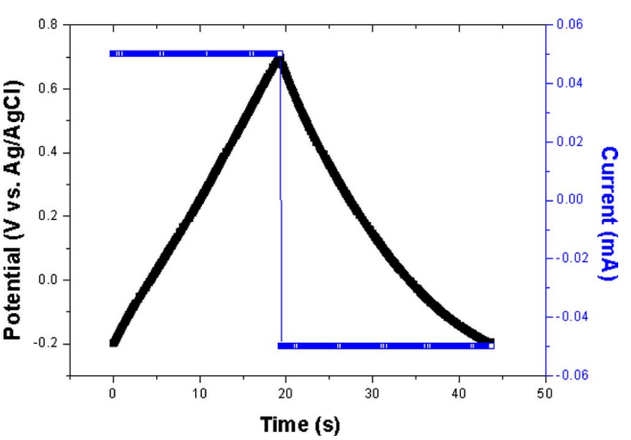

Figure 5. (Color online) Galvanostatic charge/discharge curve at a current density of 0.05 mA/cm^2 of TiO_2 nanotube arrays annealed at 400°C in 1 M HCl electrolyte.

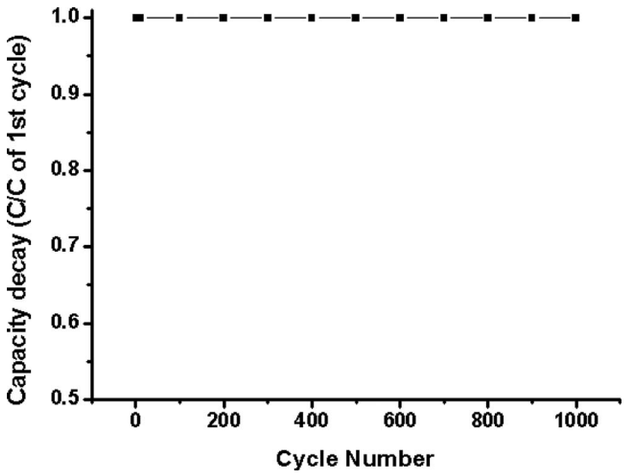

Figure 6. Discharge capacitance decay behavior vs cycle number of TiO_2 nanotube arrays annealed at 400°C in 1 M HCl electrolyte.

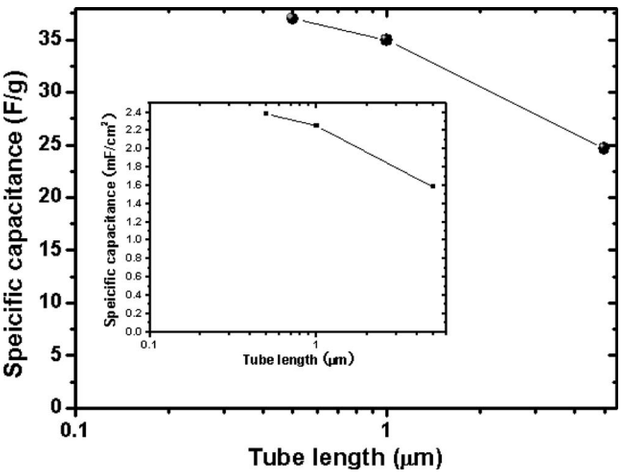

Figure 8. Specific capacitance based on the weight of the TiO_2 nanotube arrays and the geometry (inset) as a function of tube length.

increases, the disruption of the tubes as well as the breakdown of the inlet of the tubes take place, resulting in a change in the morphology of the TiO_2 nanotube arrays from a nanotubular structure to a nanoparticle structure. This is the main reason for the decrease in the surface area available to form electric double layers and the increase in the resistance, which could disturb the movement of electrons.

Figure 8 shows the dependence of the capacitance of the TiO_2 nanotube arrays on the length of the tubes. In the case of the TiO_2 nanotube arrays with a length of 4 μm, the shape of the CVs did not change and the current density increased linearly as the scan rate was increased from 5 to 50 mV/s. However, the magnitude of the specific current density was affected by the length of the tubes. It would be expected that as the tube length increases, more ions in the electrolyte would be adsorbed and the total capacitance would increase, as in the case of other EDLC materials. However, the stored charges at the end of the nanotube array would find it difficult to migrate to the current corrector, because TiO_2 is not a good electron conductor. Figure 9 shows the CVs of the TiO_2 nanotube arrays with a length of 4 μm. As increasing cell resistance, it is usually necessary to have some time interval to show the opposite discharge current after a reversed potential sweep rate in CV curves. When Fig. 9 is compared to Fig. 2a, we observe that a longer time interval is needed to observe the reverse current after the reversal of the potential sweep direction. This implies that TiO_2 nanotube arrays with a length of 4 μm have higher resistance than the 400 nm long ones.

Finally, to confirm that the use of a TiO_2 nanotube structure is the factor enabling the charge storage, we carried out the same experiments with a TiO_2 film obtained from 20 nm sized nanoparticulates. Figure 10 shows the CVs of the 5 μm thick TiO_2 nanoparticulate film annealed at 400°C in 1 M HCl electrolyte. The current density of the TiO_2 film with an irregular film structure is about 0.25 of that of the nanotubular TiO_2 film. This can be explained by the fact that the TiO_2 nanotubes can store charges more effectively than an electrode with an irregular structure under the same experiment conditions.

Conclusions

We achieved significant progress toward the goal of enhancing the charge-storage ability of TiO_2 by using vertically grown TiO_2 nanotube arrays with a controlled electrolyte and crystal structure. The unique structure of the TiO_2 nanotube arrays favors the adsorption of ions as well as the transport of charges with a very low resistance. The present investigation shows that the control of the physical structure of the electrode should be combined with the enhancement of the surface area to maximize the EDLC-type

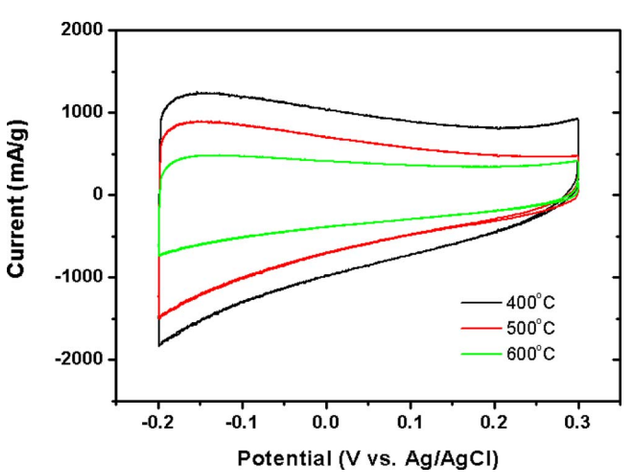

Figure 7. (Color online) CVs of TiO_2 nanotube arrays annealed at various temperatures in 1 M HCl electrolyte (scan rate: 50 mV/s).

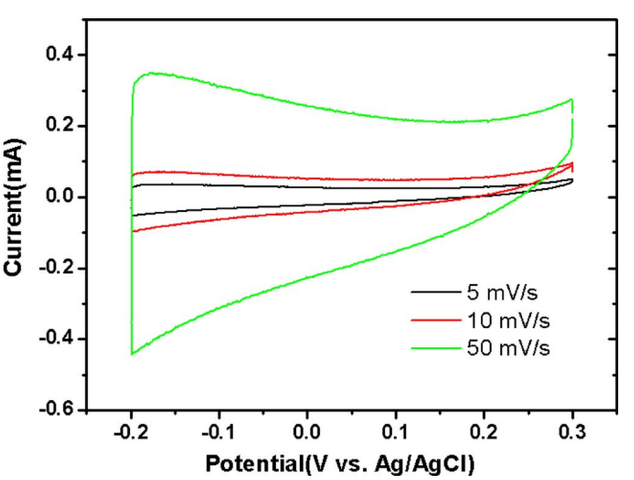

Figure 9. (Color online) CVs of 4 μm long TiO_2 nanotube arrays annealed at 400°C in 1 M HCl electrolyte.

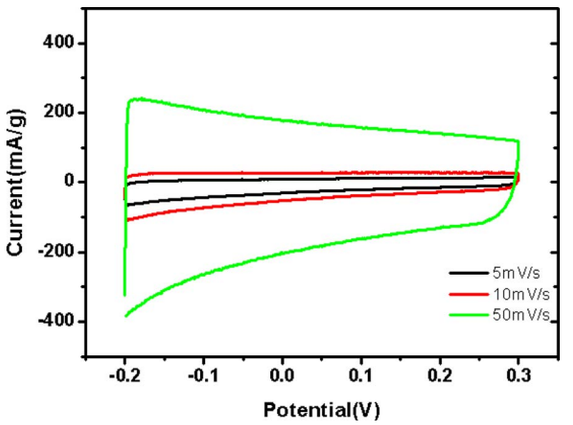

Figure 10. (Color online) CVs of 5 μm thick TiO_2 nanoparticulate film annealed at 400°C in 1 M HCl electrolyte.

charge-storage capacity. We believe that this unique EDLC-type energy-storage device has considerable potential, because it has an eight times higher density than that of AC, even though the specific capacitance of the TiO_2 nanotube arrays is about one-fourth of that of AC.

Acknowledgments

This Research was performed for the Hydrogen Energy R&D Center, one of the 21st Century Frontier R&D Program, funded by the Ministry of Education, Science and Technology of Korea.

Sungkyunkwan University assisted in meeting the publication costs of this article.

References

1. K. W. Nam, K. H. Kim, E. S. Lee, W. S. Yoon, X. Q. Yang, and K. B. Kim, *J. Power Sources*, **182**, 642 (2008).
2. D. Qu and H. Shi, *J. Power Sources*, **74**, 99 (1998).
3. O. Barbieri, M. Hahn, A. Herzog, and R. Kotz, *Carbon*, **43**, 1303 (2005).
4. A. Laforgue, P. Simson, C. Sarrazin, and J. F. Fauvarque, *J. Power Sources*, **80**, 142 (1999).
5. K. Jurewicz, S. Delpeux, V. Bertagna, F. Beguin, and E. Frackowiak, *Chem. Phys. Lett.*, **347**, 36 (2001).
6. N. L. Wu, *Mater. Chem. Phys.*, **75**, 6 (2002).
7. Y. U. Jeong and A. Manthiram, *J. Electrochem. Soc.*, **149**, A1419 (2002).
8. J. H. Park, S. W. Kim, O. O. Park, and J. M. Ko, *Appl. Phys. A: Mater. Sci. Process.*, **82**, 593 (2006).
9. E. Raymundo-Pinero, F. Leroux, and F. Beguin, *Adv. Mater. (Weinheim, Ger.)*, **18**, 1877 (2006).
10. G. Salitra, A. Soffer, L. Eliad, Y. Cohen, and D. Aurbach, *J. Electrochem. Soc.*, **147**, 2486 (2000).
11. J. H. Park, O. O. Park, K. H. Shin, C. S. Jin, and J. H. Kim, *Electrochem. Solid-State Lett.*, **5**, H7 (2002).
12. Y. G. Wang, H. Q. Li, and Y. Y. Xia, *Adv. Mater. (Weinheim, Ger.)*, **18**, 2619 (2006).
13. C. A. Grimes, *J. Mater. Chem.*, **17**, 1451 (2007).
14. G. K. Mor, O. K. Varghese, M. Paulose, K. Shankar, and C. A. Grimes, *Sol. Energy Mater. Sol. Cells*, **90**, 2011 (2006).
15. K. Zhu, N. R. Neale, A. Miedaner, and A. J. Frank, *Nano Lett.*, **7**, 69 (2007).
16. Y. Xie, L. Zhou, C. Huang, H. Huang, and J. Lu, *Electrochim. Acta*, **53**, 3643 (2008).
17. F. Fabregat-Santiago, E. M. Barea, J. Bisquert, G. K. Mor, K. Shankar, and C. A. Grimes, *J. Am. Chem. Soc.*, **130**, 11312 (2008).
18. G. K. Mor, D. K. Varghese, M. Paulose, and C. A. Grimes, *Adv. Funct. Mater.*, **15**, 1291 (2005).
19. P. Simon and T. Gogotsi, *Nature Mater.*, **7**, 845 (2008).
20. K. E. Karakitsou and X. E. Verykios, *J. Catal.*, **134**, 629 (1992).
21. J. Kiwi and M. Gratzel, *J. Phys. Chem.*, **88**, 1302 (1984).
22. P. Gouerec, H. Talbi, D. Miousse, F. Tran-Van, L. H. Dao, and K. H. Lee, *J. Electrochem. Soc.*, **148**, A94 (2001).
23. C. Arbizzani, M. Catellani, M. Mastragostino, and C. Mingazzini, *Electrochim. Acta*, **40**, 1871 (1995).
24. J. H. Park and O. O. Park, *J. Power Sources*, **109**, 121 (2002).
25. F. Beguin, K. Szostak, G. Lota, and E. Frackowiak, *Adv. Mater. (Weinheim, Ger.)*, **17**, 2380 (2005).
26. E. Y. Kim, J. H. Park, and G. Y. Han, *J. Power Sources*, **184**, 284 (2008).